The Journal of Neuroscience, April 1, 1999, 19(7):2546–2555

Noninvasive Measurements of the Membrane Potential and GABAergic Action in Hippocampal Interneurons

Jos A. H. Verheugen, Desdemona Fricker, and Richard Miles

Laboratoire de Neurobiologie Cellulaire et Moleculaire, Institut National de la Santé et de la Recherche Médicale U261, Institut Pasteur, 75724 Paris, France

Neurotransmitters affect the membrane potential (V_m) of target cells by modulating the activity of receptor-linked ion channels. The direction and amplitude of the resulting transmembrane current depend on the resting level of V_m and the gradient across the membrane of permeant ion species. V_m, in addition, governs the activation state of voltage-gated channels. Knowledge of the exact level of V_m is therefore crucial to evaluate the nature of the neurotransmitter effect. However, the traditional methods to measure V_m, with microelectrodes or the whole-cell current-clamp technique, have the drawback that the recording pipette is in contact with the cytoplasm, and dialysis with the pipette solution alters the ionic composition of the interior of the cell. Here we describe a novel technique to determine the V_m of an intact cell from the reversal potential of K^+ currents through a cell-attached patch. Applying the method to interneurons in hippocampal brain slices yielded more negative values for V_m than subsequent whole-cell current-clamp measurements from the same cell, presumably reflecting the development of a Donnan potential between cytoplasm and pipette solution in the whole-cell mode. Cell-attached V_m measurements were used to study GABAergic actions in intact CA1 interneurons. In 1- to 3-week-old rats, bath-applied GABA inhibited these cells by stabilizing V_m at a level depending on contributions from both $GABA_A$ and $GABA_B$ components. In contrast, in 1- to 4-d-old animals, only $GABA_A$ receptors were activated resulting in a depolarizing GABA response.

Key words: hippocampus; interneuron; potassium channels; cell-attached patch-clamp; membrane potential; GABA

GABA is the principal inhibitory neurotransmitter in the mammalian brain. Chloride-permeable channels, with a substantial permeability also for HCO_3^- (Bormann et al., 1987), open when GABA binds to $GABA_A$ receptors (Ozawa and Yuzaki, 1984; Gray and Johnston, 1985), whereas binding to $GABA_B$ receptors leads to G-protein-mediated K^+ channel activation (Otis et al., 1993). The resulting transmembrane currents either depolarize or hyperpolarize a postsynaptic cell, depending on the equilibrium potentials for these ions and the membrane potential (V_m) of the cell. Measuring the GABA response reversal potential (E_{GABA}) and V_m with classical methods is surprisingly difficult. Penetration with sharp microelectrodes makes a hole in the cell membrane and introduces a significant leak conductance (Spruston and Johnston, 1992), whereas whole-cell patch-clamp electrodes dialyze the cell, imposing the pipette ion concentrations on the recorded cell. Furthermore, whole-cell measurements probably underestimate V_m because an undefined Donnan potential exists between cytoplasm and pipette solution (Marty and Neher, 1995).

These problems may be avoided using a noninvasive approach, based on the reversal potential of K^+ currents through cell-attached patches, to measure V_m (Verheugen et al., 1995). When the K^+ concentration in the pipette is equal to the intracellular level, the equilibrium potential for K^+ across the membrane patch is zero. Voltage-gated K^+ currents [K(V)], elicited via the patch electrode, will reverse direction when the pipette potential ($-V_h$) equals V_m. Repetitive measurements of K(V) reversal in the cell-attached mode may then be used to follow fluctuations in V_m. Furthermore, changes in K(V) reversal during exposure to GABA and selective agonists of $GABA_A$ and $GABA_B$ receptors can provide estimates of respectively E_{GABA}, $E_{GABA\text{-}A}$, and $E_{GABA\text{-}B}$, or at least (in the case other conductances still significantly contribute in setting V_m) of their polarity with respect to the resting V_m.

The relation between E_{GABA} and V_m of hippocampal interneurons is of particular interest. GABA-mediated membrane currents in hippocampal neurons may be depolarizing in young animals (Mueller et al., 1984; Ben-Ari et al., 1989) and under certain conditions in adult animals (Alger and Nicoll, 1979; Thompson and Gähwiler, 1989; Michelson and Wong, 1991). GABA-mediated depolarizing postsynaptic potentials (Kaila et al., 1997) could function as a source of positive feedback and so synchronize discharge in interneuron networks (Michelson and Wong, 1991). Interneuron synchronization has been implicated in the generation of neonatal hippocampal oscillations (Strata et al., 1997) and of the 40 Hz gamma rhythm in adult hippocampus and cortex (Whittington et al., 1995). We therefore studied the GABA actions on intact interneurons from rats at different stages of postnatal development using the reversal potential of cell-attached K(V) currents as monitor of V_m.

MATERIALS AND METHODS

Hippocampal slice preparation. Rats aged between 1 and 21 d were anesthetized by intraperitoneal injection of a ketamine–chloral hydrate solution (5 and 18%, respectively; 1 ml/200 gm). Under deep anesthesia, the vascular system was perfused through the heart with an ice-cold low Ca^{2+} solution containing (in mM): 130 NaCl, 2.7 KCl, 20 $NaHCO_3$, 0.4 $CaCl_2$, 1 $MgCl_2$, 1.3 NaH_2PO_4, and 25 glucose, equilibrated with 5% CO_2 and 95% O_2. After perfusion, the brain was removed, and sagittal slices of 200–300 μM were cut from the middle third of the hippocampus

Received Nov. 30, 1998; revised Jan. 21, 1999; accepted Jan. 25, 1999.

This work was supported by the Human Frontiers Science Organization, the National Institutes of Health (MH54671), and Institut National de la Santé et de la Recherche Médicale. We thank I. Cohen for writing the data analysis program.

Correspondence should be addressed to Dr. Jos A. H. Verheugen, Laboratoire de Neurobiologie Cellulaire et Moleculaire, Institut Pasteur, 25 rue du Dr Roux, 75724 Paris cedex 15, France.

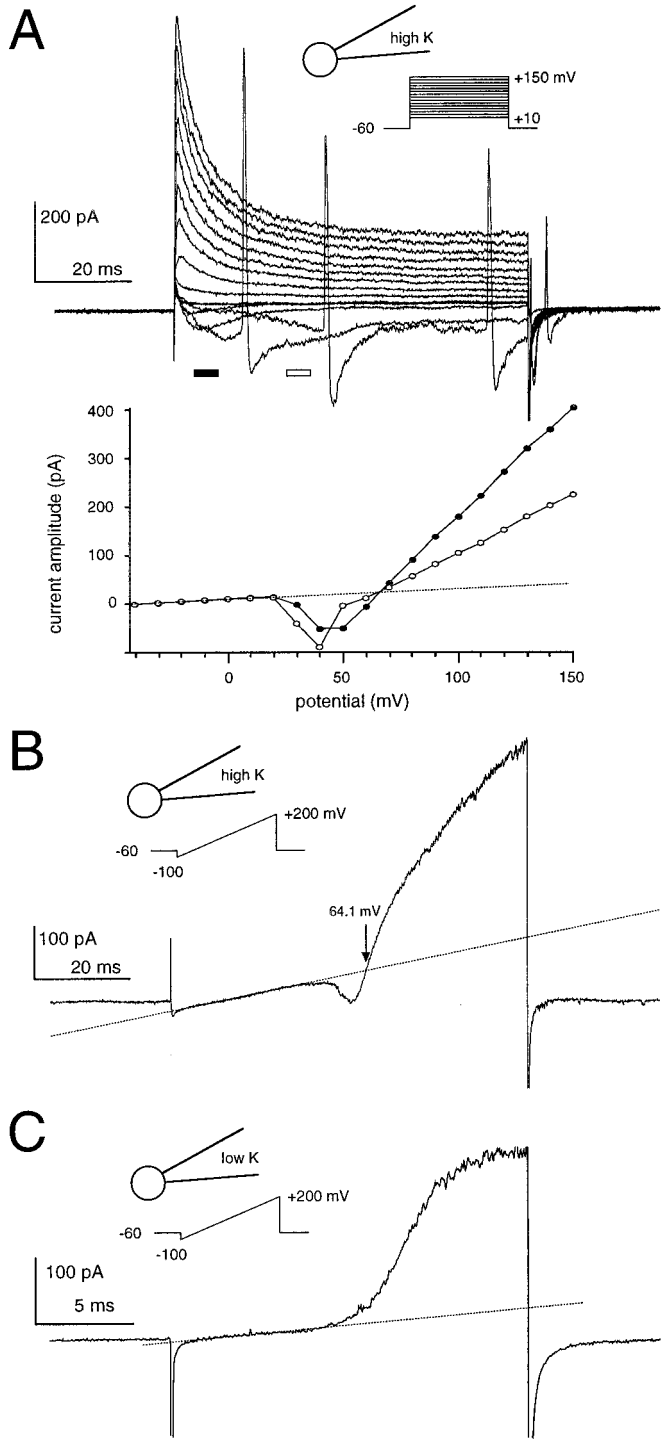

Figure 1. Voltage-gated K^+ currents measured in cell-attached patches of CA1 interneurons. *A* shows currents activated by applying depolarizing voltage steps, and *B* shows the response to a voltage ramp applied to the same cell, with a pipette solution containing 155 mM K^+. *A*, The inward K^+ current caused the generation of action currents in this cell (Lynch and Barry, 1989). At more depolarized potentials the current became outward and consisted of a transient and sustained component. Current–voltage curves (below), constructed from the average current amplitude at the times indicated by the *black* and *white bars* in the *top panel*, show that the K^+ current was superimposed on a linear leak (*dotted lines*) and reversed polarity from inward to outward between +60 and +70 mV. Note that the reversal potential of the voltage-gated current is independent of the relative contributions of the transient and sustained component. *B*, A voltage ramp stimulation gave a similar *I–V* profile, but no action currents were generated because of a reduced charge flux. With symmetrical K^+, the current reversal at V_h = +64 mV indicated a membrane potential of −64 mV. *C*, With a low K^+ pipette solution, in which 135 mM K^+ was replaced with the impermeant cation *N*-methyl-D-glucamine, the voltage-gated current was outward for all voltages beyond the activation threshold, demonstrating its K^+ selectivity.

using a vibratome (DTK-1000 microslicer; Dosaka, Kyoto, Japan). Slices were allowed to recover for at least 1 hr in the above solution with 2 mM $CaCl_2$ ("extracellular solution"). For recordings, slices were placed in a chamber mounted on the stage of a microscope (Nikon Optiphot with a 40×, 0.55 NA objective). They were held in place by a nylon grid and continuously superfused with the oxygenated extracellular solution at room temperature (24–26°C).

Cell-attached and whole-cell patch-clamp recording. Hippocampal interneurons in stratum radiatum of the CA1 area were visualized using a CCD camera (Hamamatsu C3077) with light filtered to pass visible and infrared. Pipettes (Clark Electromedical Instruments, Pangbourne, UK; GC150 borosilicate glass) with a resistance of 2–6 MΩ were filled with a high K^+ solution consisting of (in mM): 120 KCl, 11 EGTA, 1 $CaCl_2$, 2 $MgCl_2$, 10 HEPES, adjusted to pH 7.25 with 35 mM KOH (final K^+ concentration 155 mM) and to 310 mOsmol with 20 glucose, unless stated otherwise. The junction potential between pipette and extracellular solution (<3 mV as measured according to Neher, 1992) was nulled by the voltage-offset of the amplifier (Axopatch 200A) before establishing the seal and was not further corrected. Seal formation was performed under visual control, maintaining positive pressure in the patch electrode when entering into the slice. Stimulation protocols were implemented and data acquired with pClamp6 software (Axon Instruments, Foster City, CA). Currents were low-pass filtered at 5 kHz and digitized at 50–85 kHz.

Using the reversal potential of K^+ currents through cell-attached patches as a monitor of the membrane potential. The method to measure V_m from cell-attached K^+ currents was adapted from Verheugen et al. (1995) for human T lymphocytes. With a 155 mM K^+ pipette solution, which is the estimated intracellular K^+ concentration (Hille, 1992), the equilibrium potential for potassium (E_K) across the patch is ~0 mV, and K^+ currents will reverse when the pipette potential cancels V_m out. Therefore, the holding potential (V_h, note that for cell-attached recording $V_h = -V_{pipette}$) at which the K^+ current reverses direction gives a direct quantitative measure for the cell's membrane potential, V_m (at K^+ reversal $V_m + V_h = E_K \approx 0$ mV). With this approach, differences between intracellular and pipette K^+ concentration would result in errors in the V_m estimate, which will be too negative when $[K^+]_i < [K^+]_{pipette}$. However, with a $[K^+]_{pipette}$ of 155 mM a difference of, for example, 15 mM would result in an error of $RT/F \cdot ln(155/140) < 3$ mV. Depolarizing voltage ramps (from $V_h = -100$ to +200 mV) were applied to activate voltage-gated K^+ channels and to establish the K^+ current reversal potential. Between stimulations, the patch was held at −60 mV hyperpolarized with respect to V_m to remove possible voltage-dependent "steady-state" inactivation from the K(V) channel at the physiological V_m. For analysis of currents evoked by ramp stimulation, a correction was made for a leak component by linear extrapolation of the closed level below the threshold for activation of the voltage-gated current (Fig. 1*A*,*B*, *dotted lines*). In patches that did not contain K(V) channels, the leak current was virtually linear in the entire potential range of the voltage ramp (data not shown). Goodness of the linear fit of the leak and determination of the reversal potential from the intersection between the extrapolated fit and K^+ current were visually confirmed for each individual current trace. Data were analyzed using Axograph 3 (Axon Instruments) or in Labview (National Instruments) using an automated procedure written by Ivan Cohen.

Pharmacology. GABA, muscimol, baclofen, and TTX (all from Sigma, St. Louis, MO) and NBQX and APV (Tocris, Bristol, UK) were made up as 1000× concentrated stocks and diluted to their final concentrations in the external solution before use. The compounds were applied via bath perfusion. Using a gravity-driven perfusion system, the bath solution completely changed in ~30 sec.

RESULTS

V_m measurements from cell-attached K(V) currents

The membrane potential of interneurons in the stratum radiatum of the CA1 area of hippocampal slices was estimated from the

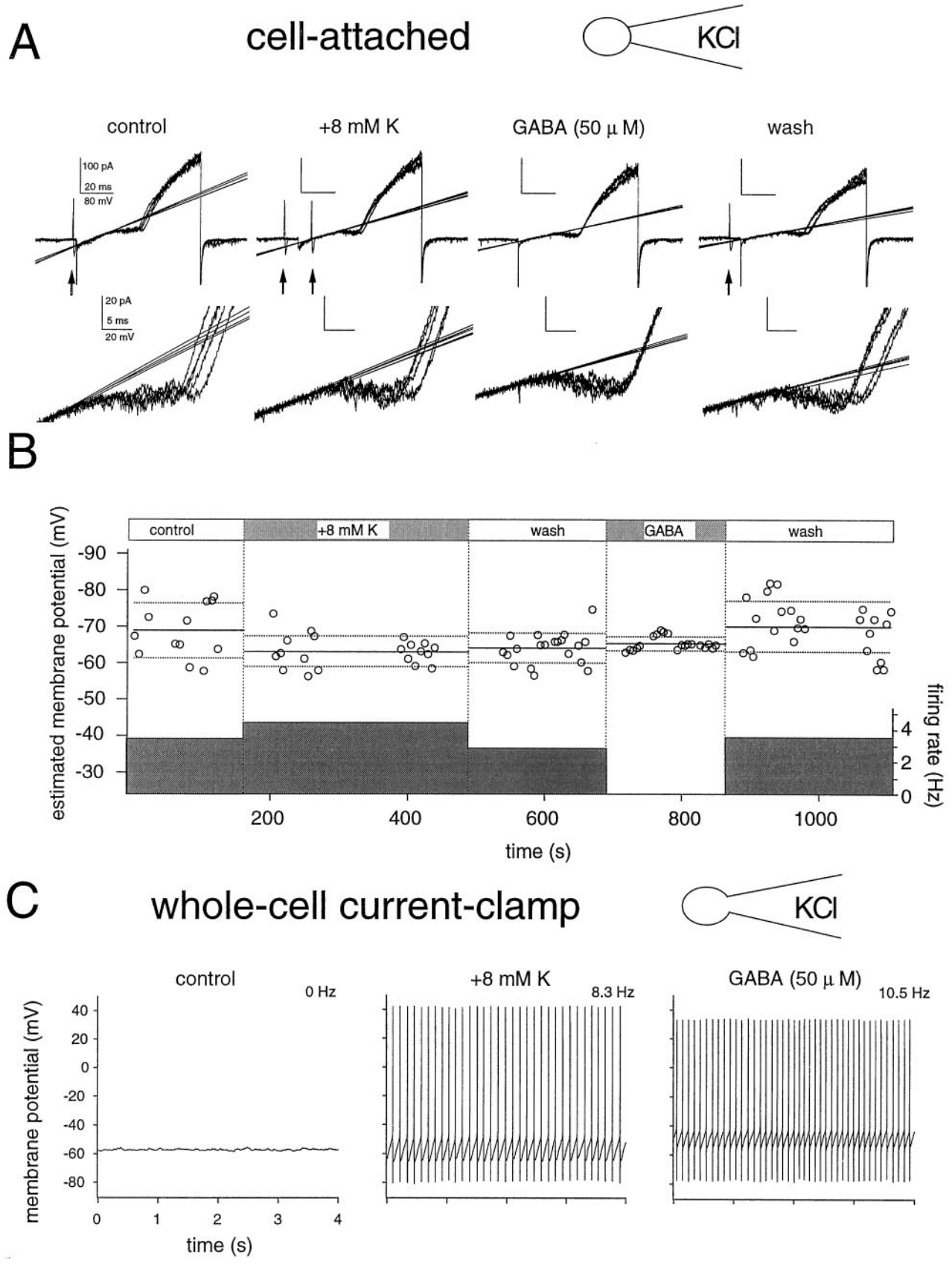

Figure 2. Differences between cell-attached and whole-cell V_m measurements. *A*, Determination of K^+ current reversal, and hence membrane potential, from a CA1 interneuron after exposure to high external $[K^+]$ and to GABA (50 μM). This cell discharged spontaneously, giving rise to action currents visible in the cell-attached record (*arrows*). For each condition, five consecutive current traces recorded at 2 sec intervals are shown. *Bottom panels* show the inward K(V) and its reversal in greater detail. *B*, Plot of V_m determinations (*circles*; for each condition average V_m and SD *(Figure legend continues)*

reversal potential of voltage-gated K^+ currents activated by command potentials applied via a cell-attached pipette (Fig. 1). This technique permits control of the timing of measurements and is more precise than estimates from changes in amplitude of spontaneous K^+ channel open events (Zhang and Jackson, 1993; Soltesz and Mody, 1994; Verheugen et al., 1995). Voltage steps applied to somatic patches of interneurons elicited K^+ currents [$I_{K(V)}$] with a transient (inactivation time constant, 12.9 ± 4.0 msec) and a sustained component (Fig. 1*A*) corresponding to the I_A and delayed rectifier components of whole-cell K^+ currents (Zhang and McBain, 1995). With 155 mM K^+ in the pipette, K(V) currents were activated between −10 and +50 mV (relative to V_m) and were initially inward reaching a maximum amplitude of 32 ± 35 pA. They reversed at potentials between +55 and +90 mV, and outward currents of 279 ± 204 pA were attained at +140 mV.

Voltage ramp stimulation produced similar *I–V* relations to those derived from responses to current steps (Fig. 1*B*). The currents were selective for K^+ because they were outward over the entire voltage range with pipettes containing low K^+ (20 mM; Fig. 1*C*). Furthermore, there were no differences in depolarization evoked currents when the pipette solution contained Cl^- or gluconate as the main anion ($p > 0.1$; data not shown).

Ramp stimuli were routinely used to determine the K(V) current reversal potential and hence V_m. A correction was made for the linear leak current evident at potentials below the K(V) current threshold (Fig. 1, *dotted lines*). Short duration (15–20 msec) ramps were preferred because they minimized transmembrane charge flux while still producing close to maximal activation of the K(V) current (Figs. 2-5). Ramp stimuli could be repeated at frequencies up to 1 Hz without significant accumulation of use-dependent K^+ current inactivation. The mean resting V_m of CA1 interneurons, estimated with the cell-attached approach, was −73 ± 9 mV ($n = 50$) ranging between −59 and −93 mV.

Large fluctuations in V_m, with an amplitude of 21 ± 6 mV, were apparent in a subset of the cells ($n = 22$ cells). Action currents were usually visible in the cell-attached records from these neurons (Fig. 2*A*). The afterhyperpolarizations after the action potentials (APs) (which may be of large amplitudes in CA1 interneurons; Parra et al., 1998) contributed to the fluctuations, which shrank to about half their size during periods without APs (see also Fig. 4*A*). Depolarizing the cells by increasing extracellular [K^+] increased the rate of action current generation but reduced fluctuations of V_m because of the smaller amplitude of the AHPs (Fig. 2*B*). The primary origin of the fluctuations are spontaneously occurring excitatory synaptic events because both the APs and residual fluctuations were largely blocked by applying NBQX/APV to the bath (see below). Bath application of GABA (50 μM) also considerably reduced fluctuations in V_m (Fig. 2*B*). The generation of action currents invariably ceased, and voltage changes caused by spontaneous synaptic events were presumably considerably reduced because of the shunting action of the GABA-dependent increases in Cl^- and K^+ conductances. The residual variability of V_m estimates in the presence of GABA was close to ±2 mV, which gives an index of the resolution of the method.

To compare measurements of V_m from K^+ current reversal in cell-attached records with those determined using the traditional whole-cell current-clamp configuration, the two methods were applied sequentially in experiments on 21 cells. Several differences between the two approaches were apparent (Fig. 2*C*).

First, values for membrane potential were systematically different. With a high Cl^- pipette solution, values for V_m from the cell-attached technique were on average 15 ± 6 mV ($n = 21$) more hyperpolarized than those measured subsequently from the same cell in current-clamp mode after break-in to the whole-cell configuration (Fig. 2*C*, *left panel*). A similar difference (13 ± 9 mV; $n = 10$) was observed when the pipette solution contained a low Cl^- concentration (14 mM Cl^-/130 mM gluconate). Second, neuronal discharges were often modified. Action currents were apparent in cell-attached records from the cell shown in Figure 2, but firing ceased once the whole-cell configuration was established. Inversely, cells that were silent in cell-attached records sometimes began to discharge after the transition to the whole-cell mode. The changes seemed not to result from dialysis of the cellular cytoplasm with the pipette solution, because they occurred immediately after the membrane was broken and did not depend on the composition of the pipette solution. This point was confirmed by examining the time course of changes in membrane potential and firing after break-in during GABA application, in experiments with pipette solutions containing either a high or a low Cl^- concentration. As expected, GABA excited cells recorded in the whole-cell mode with a high Cl^- pipette solution (Fig. 2*C*, *right panel*), whereas it had an inhibitory action when cells were recorded with a low Cl^- solution (data not shown). However, these actions did not occur immediately but had a slow onset that reached a steady-state 0.5–2 min after break-in as expected if they resulted from intracellular perfusion. These results therefore suggest that the establishment of whole-cell recording alone can modify neuronal excitability, possibly by changing the activation state of voltage-gated channels.

Of note, the observation that intracellular perfusion with a high Cl^- solution affects V_m differently under control conditions and after exposure to GABA indicates that in CA1 interneurons Cl^- is not the principal ionic species involved in setting the resting level of V_m.

Origin of the difference in cell-attached and whole-cell V_m estimates

Two possible explanations were considered to explain the difference in cell-attached and whole-cell estimates for V_m. First, it could result from an artifactual shift in V_m induced by the ramp stimulation in cell-attached recordings. Determinations of V_m made using a second independent method based on spontaneous single K^+ channel openings seem to exclude this explanation.

In some patches, spontaneous openings of non-voltage-activated K^+ channels were apparent in addition to the K(V) current gated by membrane depolarization. Figure 3*A* shows

←

are indicated by *solid* and *dotted lines*, respectively) and the mean firing frequency (*shaded bar*) in the presence of high K^+ and GABA. Increasing extracellular [K^+] from 2.5 to 10.5 mM caused a depolarization, and the firing rate increased. In contrast, during GABA application V_m stabilized, and the generation of action currents ceased. *C*, V_m measured subsequently from the same cell in the whole-cell current-clamp mode was more depolarized. No spontaneous AP activity was seen, and membrane potential was stable within 2–3 mV. Increasing $[K^+]_o$ and GABA application both strongly excited the cell. The pipette solution contained 120 mM Cl^-, and the interneuron was recorded from a slice obtained from a 17-d-old rat.

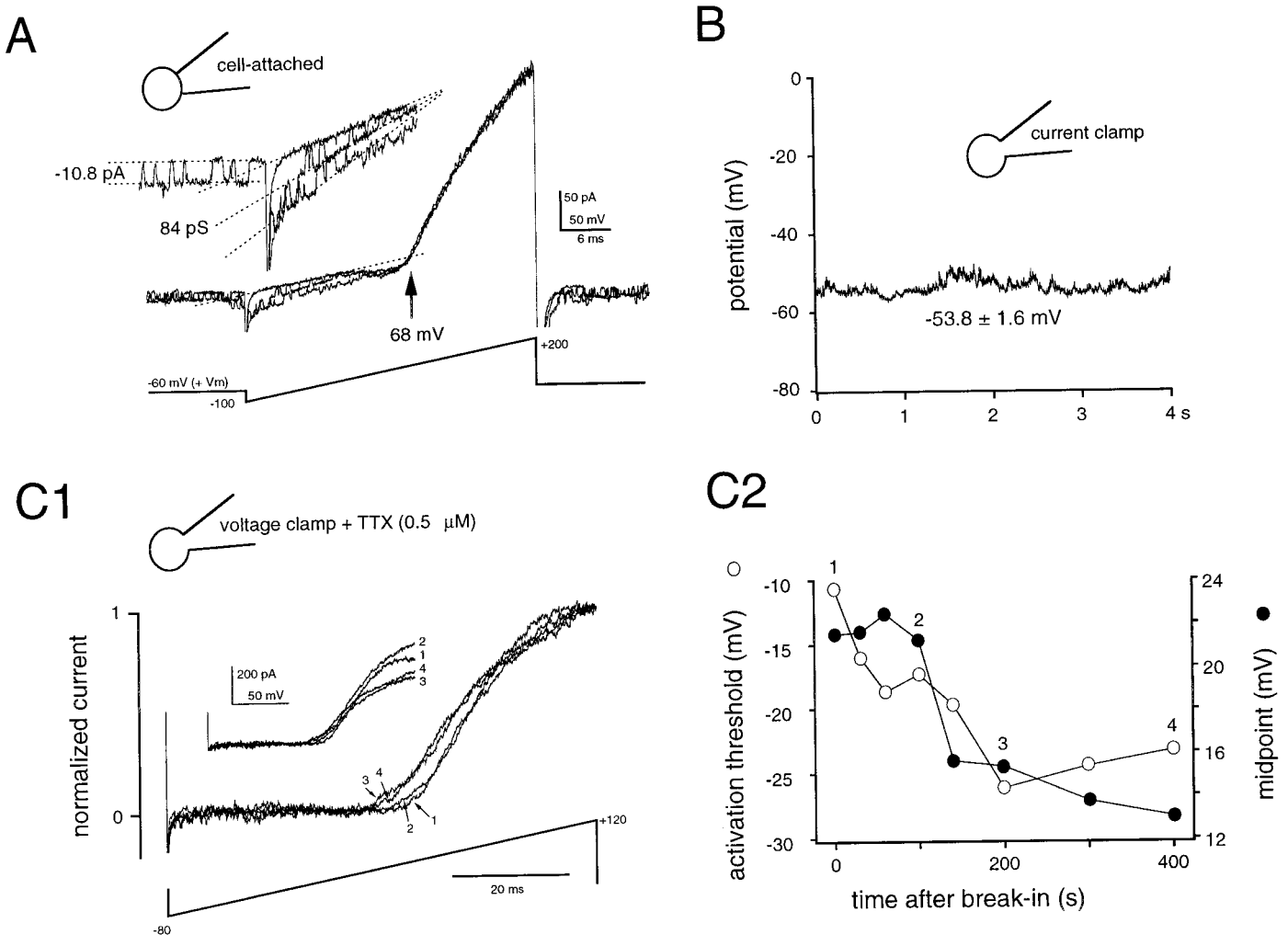

Figure 3. The Donnan potential between cytoplasm and pipette in the whole-cell mode can account for the difference in cell-attached and current-clamp V_m estimates. *A*, Three superimposed cell-attached current traces from a cell with spontaneous single-channel activity ($K_{"ATP"}$). Two independent estimates for V_m can be obtained from these records. With the single-channel amplitude at $V_h = -60$ mV and the single $K_{"ATP"}$ channel conductance calculated from the slope of the open levels during the voltage ramp stimulation, the driving force for K^+ flux ($V_{patch} - E_K$; with $V_{patch} = V_h + V_m$ and $E_K \approx 0$ mV) amounts to 10.8 pA/84 pS = 128.6 mV at $V_h = -60$ mV, yielding an estimated V_m of −68.6 mV. The value determined for V_m from reversal of the macroscopic K(V) current was −69.2 mV. The close agreement between these two values indicates that the ramp stimulation does not significantly affect V_m. *B*, Subsequent whole-cell current-clamp measurement in the same cell gave a value of -53 ± 3 mV for V_m. *C1*, Evidence for a change in Donnan junction potential with time after the establishment of whole-cell recordings in the same cell as *A* and *B*. Whole-cell K(V) currents activated by ramp stimuli showed a gradual hyperpolarizing shift in voltage dependence. *C2*, Both the activation threshold (*open circles*) and the voltage corresponding to the half-maximal current (*filled circles*) shifted by approximately −15 mV during the first 4–8 min after break-in. Current traces were normalized to compensate for a partial rundown of the K(V) current (*C1*, *inset*). The slice was from a 15-d-old rat.

spontaneous activity of a channel with conductance and inward rectification properties similar to those of an ATP-sensitive K^+ channel described in cortical cells (Ohno-Shosaku and Yamamoto, 1992; Sakura et al., 1995). These current records provide two independent means to measure V_m. Dividing the single-channel amplitude of $K_{"ATP"}$ by its conductance, calculated from open states during ramp stimuli (see Fig. 3, legend), gives the driving force for current flowing through the channel. The reversal potential was identical for both channels, indicating that they are equally K^+ selective, and the driving force is therefore the difference between E_K and the patch potential. In the records shown in Figure 3*A*, the single-channel amplitude at −60 mV for the $K_{"ATP"}$ channel indicates a patch potential of −128.6 mV, and thus a V_m of −68.6 mV (assuming $E_K = 0$ mV). This value was very similar to that determined from the reversal potential of the "macroscopic" voltage-gated K^+ current (−69.2 mV). This good agreement suggests strongly that neither the inward K(V) component nor the leak current induced by the voltage ramp significantly affected V_m. In eight patches, estimates for V_m using these two distinct approaches always converged within 0–3 mV.

A second explanation for the difference between cell-attached and whole-cell measurements of V_m might be the existence of a Donnan potential between the pipette solution and the cytoplasm. Such a potential would lead to an underestimation of the V_m in whole-cell experiments (Barry and Lynch, 1991; Marty and Neher, 1995). The gradual disappearance of a Donnan potential as large anions diffuse out of the cell has been monitored as a shift in the apparent voltage dependence of whole-cell currents (Marty and Neher, 1995). In interneurons, depolarizing ramps were applied at regular intervals after break-in to the whole-cell mode to test whether such changes in the voltage dependence of the K(V) current occurred. In the cell shown in Figure 3, *A* and *B*, the

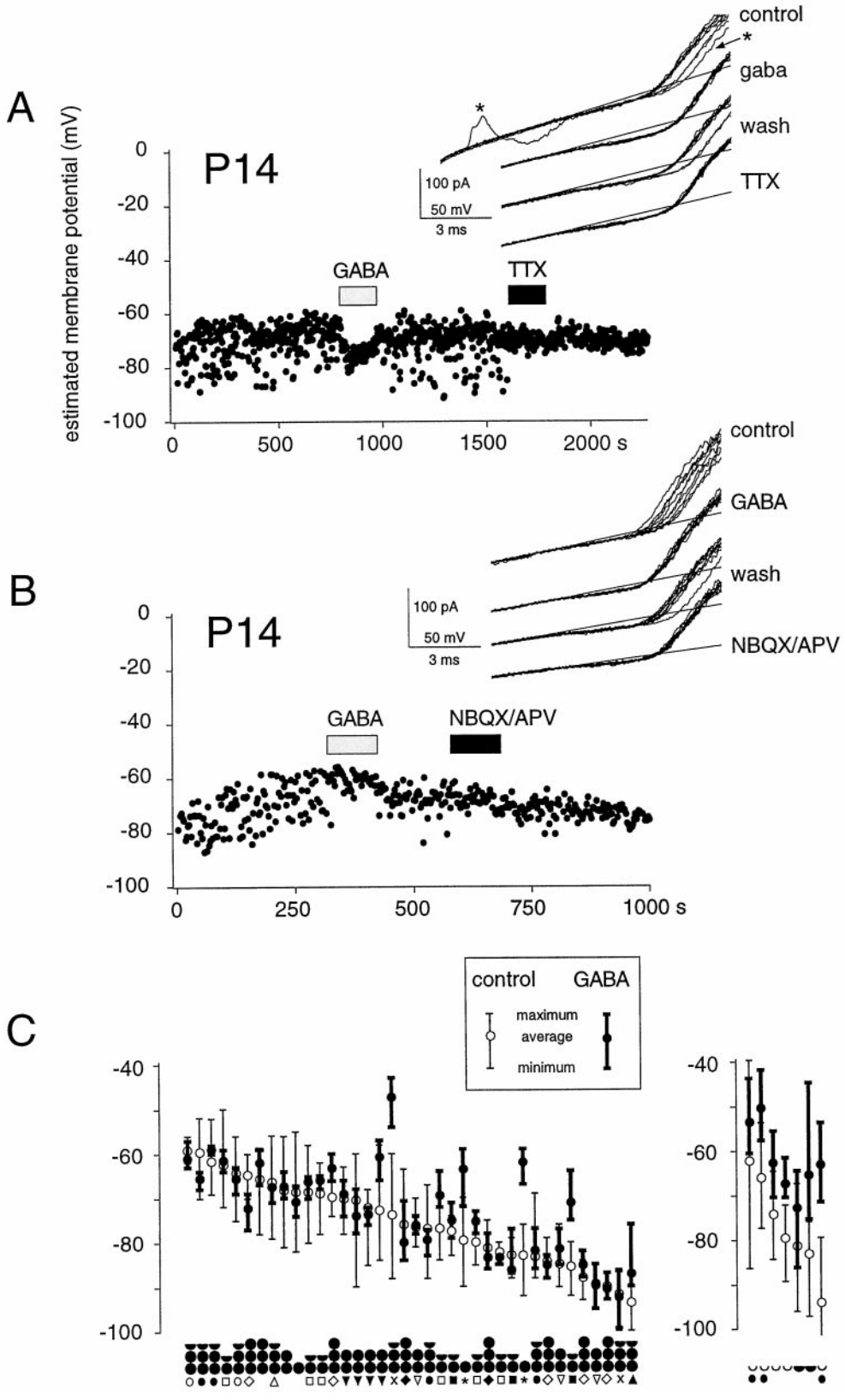

Figure 4. Effects of GABA receptor activation on the V_m of intact CA1 interneurons. V_m of two CA1 interneurons under control conditions and in the presence of bath-applied GABA and TTX (*A*) and GABA and NBQX/APV (*B*) monitored from the cell-attached K(V) current reversal. V_m of both interneurons fluctuated spontaneously, which was associated with AP activity (see current trace in *A*). The fluctuations were largely suppressed by TTX (0.5 μM; *A*) or by NBQX/APV (20 and 100 μM; *B*), indicating that they arise from excitatory input to the cell, although the AHPs after action potentials contribute to the hyperpolarizing deflections (*A*, *asterisks*). The principal effect of bath-applied GABA in P7–P21 animals is a stabilization of the V_m, usually at a level that is not significantly different (*A*) or slightly depolarized (*B*) from the average control level. The *inset* shows for each condition the reversal of K(V) currents from 10 consecutive cell-attached responses to ramp stimuli applied at 2 sec intervals. *C*, Summary of GABA effects on interneurons from P7–P21 (*left*) and P1–P4 rats (*right*). In the older animals, GABA caused V_m to stabilize at a potential close to control level, whereas in young animals it induced a membrane depolarization. Cells are aligned according to the average V_m. Minimum and maximum V_m levels are indicated in the presence and absence of GABA. The mean V_m of cells in the two age groups was not significantly different ($p > 0.1$). The *black circles* under the graph indicate the approximate age of the animal, with each postnatal week corresponding to one circle; an *empty half circle* indicates 1-to 2-d-old rats. Cells originating from the same animal are identified with *symbols*.

difference between values for V_m determined using the cell-attached and whole-cell techniques was approximately −15 mV. In the first 20 min after the onset of whole-cell recording, the K(V) current–voltage relation shifted by the same order of magnitude (Fig. 3*C*). The mean shift in the K(V) activation threshold, in the period of 5–20 min after break-in was −16 ± 10 mV (n = 5 cells; range, 3–27 mV), which corresponded to 80 ± 30% of the difference in V_m estimates. In the absence of TTX, which was

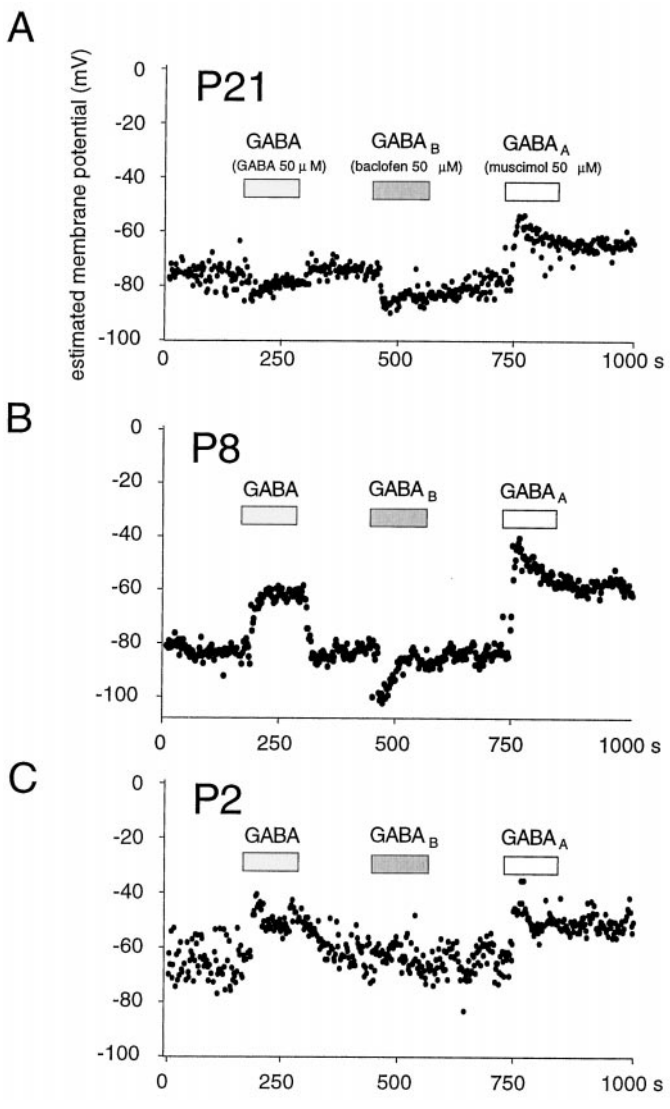

Figure 5. Age dependence of the effects of activating $GABA_A$ and $GABA_B$ receptors. Each experiment shows membrane potential responses to application of GABA (50 μM), to activation of $GABA_B$ receptors by baclofen (50 μM), and to the activation of $GABA_A$ receptors by muscimol (50 μM). *A*, *B*, In animals older than P7, activation of $GABA_A$ receptors induced a depolarizing response, whereas $GABA_B$ receptor activation induced a hyperpolarization. The effects of GABA were a balance depending on combined responses of both receptor subtypes. *C*, In interneurons from young (P1–P4) animals, $GABA_B$ receptor activation had no effect, and both GABA and muscimol induced depolarizing responses.

used in the above whole-cell experiments to isolate the voltage-gated K^+ currents, similar shifts in voltage dependence of Na(V) currents after break-in were observed ($n = 4$ cells; data not shown).

Effects of GABAergic agonists on V_m in intact interneurons

During experiments to examine Donnan shifts in voltage dependence of K^+ currents, a partial rundown of the peak current was usually apparent (Fig. 3*C*). In contrast, the K(V) current never ran down in the cell-attached mode. This difference presumably reflects the better conservation of the cytoplasmic environment in cell-attached recordings. Cell-attached measurements of V_m might therefore offer significant advantages in studies on neurotransmitters whose actions depend critically on the cytoplasmic contents. One such neurotransmitter is GABA, which opens Cl^-/HCO_3^--permeable channels and activates a G-protein-mediated K^+ conductance, by activation of $GABA_A$- and $GABA_B$-linked ion channels, respectively. We therefore used the cell-attached approach to study the effects of GABA on CA1 interneurons.

Exogenous GABA (50 μM) and the selective $GABA_A$ and $GABA_B$ agonists muscimol (50 μM) and baclofen (50 μM) were applied by bath perfusion while monitoring V_m from the reversal of cell-attached K^+ currents (Fig. 4). Because GABAergic actions on pyramidal cells are reported to change with age (in rabbit: Mueller et al., 1984; in rat: Ben-Ari et al., 1989; Zhang et al., 1991; Chen et al., 1996; Owens et al., 1996), slices were used from animals at various periods after birth. Indeed, there were significant differences in responses to GABA of interneurons from young [postnatal day 1–4 (P1–P4)] and older (P7–P21) animals.

In the older age group, GABA hyperpolarized a small minority of the interneurons (5%; $n = 39$). More cells (26%) depolarized in the presence of GABA (Fig. 4*B*). However, in the vast majority of the cells (69%), no significant change in the average level of V_m occurred (Fig. 4*A*). These qualitatively different responses to GABA could be observed in interneurons derived from the same animal (Fig. 4*C*). Irrespective of the change in average V_m, GABA tended to stabilize interneuron membrane potential (Fig. 4*A,B*; see also Fig. 2). This effect was particularly striking in cells with strong V_m fluctuations and spontaneous firing activity, which invariably ceased in the presence of GABA (Figs. 2, 4*C*).

As described above, these membrane potential fluctuations were usually associated with action current generation and, as expected, were considerably reduced in the presence of a 0.5 μM concentration of the Na(V) channel blocker TTX (Fig. 4*A*). It seems probable that action potential generation by these interneurons was largely dependent on excitatory synaptic inputs because exposure to the excitatory amino acid antagonists NBQX (20 μM) and APV (100 μM) also significantly reduced membrane potential fluctuations (Fig. 4*B*). These data suggest therefore that the primary effect of simultaneous strong activation of both $GABA_A$ and $GABA_B$ receptors is to stabilize V_m of interneurons from P7–P21 rats, presumably by a shunting action.

In contrast to the relatively small effects on the average level of V_m in older animals, GABA invariably depolarized interneurons from animals aged between 1 and 4 d (Figs. 4*C*, 5*C*). In young animals its effect in stabilizing fluctuations in V_m was much less pronounced (Fig. 4*C*). However, in young animals, as in old, depolarizations induced by GABA rarely caused an excitation. Only in one of seven P1–P4 cells, the depolarization induced by GABA was sufficient to evoke APs.

The contribution of different subtypes of GABA receptors was examined by comparing the effects on V_m of GABA (50 μM), muscimol (50 μM) to activate $GABA_A$ receptors, and baclofen (50 μM) to activate $GABA_B$ receptors (Fig. 5). These experiments revealed that responses to GABA depended on the balance between contributions of the $GABA_A$-activated Cl^-/HCO_3^- conductance and the $GABA_B$-activated K^+ conductance. Thus, in interneurons from P7–P21 rats, the level at which V_m stabilized in the presence of GABA (-69 ± 12 mV from a resting level of -78 ± 9 mV; $n = 15$) was between the hyperpolarized level reached in the presence of baclofen (-89 ± 8 mV) and the depolarized response to muscimol (-54 ± 8 mV; Fig. 5*A,B*). Both

the $GABA_B$- and $GABA_A$-induced changes in V_m relaxed during prolonged receptor activation, presumably because of redistribution of permeant ions (Kaila, 1994). In contrast, GABA responses remained usually stable during maintained applications.

Whereas GABA and muscimol had different effects on V_m in P7–P21 rats, in interneurons from young animals these two agonists caused similar depolarizations, to -54 ± 8 mV and -55 ± 8, respectively, from a resting level of -74 ± 14 mV ($n = 5$). This difference may be explained by an absence of functional $GABA_B$ receptors in neurons from P1–P4 animals because baclofen had no effect on V_m (Fig. 5*C*). Thus, in these cells, exogenous GABA only increases the Cl^-/HCO_3^- permeability of the membrane, resulting in a depolarization. Of note, the level of V_m reached in the presence of muscimol was the same for both age groups. Like the depolarizing GABA response in young animals, the depolarization induced by muscimol in both young and older animals was rarely excitatory. Action currents were generated by the muscimol-induced depolarization in one of five P1–P4 cells and in two of 15 P7–P21 cells.

DISCUSSION

Measurements of neuronal membrane potential and neurotransmitter actions are more difficult than commonly admitted. We have shown that the reversal of voltage-gated K^+ currents elicited in cell-attached patches can provide a noninvasive way to determine these parameters. This technique has several advantages: (1) it provides a local measure of V_m, at the site of the patch; (2) it does not disrupt the cytoplasmic environment; and (3) it avoids Donnan junction potential problems. In this study we validated the technique and used it to examine GABA actions on hippocampal interneurons.

Validation of the technique

Variations in amplitude of cell-attached currents passing through single potassium channels have previously been used to infer changes in V_m in neurons in response to GABA (Zhang and Jackson, 1993; Soltesz and Mody, 1994) and in T lymphocytes during Ca^{2+} signaling (Verheugen and Vijverberg, 1995). This technique has the disadvantage that measurements are limited to periods when channels are open. For instance, the Ca^{2+}-activated K^+ channels used in these studies open only when $[Ca^{2+}]_i$ is higher than normal, a state that is usually associated with membrane hyperpolarizations as a consequence of this increase in K^+ conductance (Verheugen and Korn, 1997). In contrast, the voltage-gated K^+ channels used to determine the K^+ current reversal potential in the present study could be opened by voltage steps applied to the patch at will, independent of intracellular conditions. Furthermore, while changes in single-channel amplitude provide relative estimates of V_m, an absolute value of V_m is obtained from the K^+ current reversal (Verheugen and Vijverberg, 1995).

One potential problem is that the ion current through the K(V) channels could result in a change of V_m (Fig. 1*A*). However, because the patch current is, by definition, zero at the reversal potential, this point should be accurate. The use of fast voltage ramps to determine K(V) reversal further reduces transmembrane charge fluxes. Similar values for V_m estimates from macroscopic and single-channel currents (Fig. 3*A*) provide additional evidence that under the present conditions the cell-attached currents had little influence on V_m.

Another potential source of error might be a mismatch between the $[K^+]$ used in our pipette solution and the effective cytoplasmic $[K^+]$. Deviations from symmetrical K^+ would result in an E_K across the patch different from 0 mV. However, based on the Nernst equation we calculate that an error of for instance 15 mM in the choice of pipette $[K^+]$ would result in a systematic error of only 3 mV in our determinations of V_m.

The V_m values obtained from the cell-attached K(V) reversal were on average 15 mV more negative than those measured subsequently in whole-cell current-clamp recordings in the same neuron. The existence of a Donnan potential between the cytoplasm and pipette solution immediately after break-in to the whole-cell mode probably accounts for this difference. During the first 5–20 min after the whole-cell configuration was established, the voltage dependence of voltage-gated currents shifted by a similar value (Fig. 3*C*) most likely corresponding to equilibration between the cytoplasm and the recording pipette and consequent dissipation of the Donnan potential (Marty and Neher, 1995). Therefore, the more negative cell-attached V_m estimates seem likely to be more accurate than the values derived from whole-cell records.

Another advantage of this technique is that the cytoplasmic environment is preserved. In contrast, in the whole-cell technique the pipette solution controls over time the intracellular content, disturbing physiological ion gradients and diluting intracellular factors. The perforated patch technique, which uses antibiotics to render cell membranes permeant to monovalent ions (e.g., nystatin; Horn and Marty, 1988) or selectively to small cations (gramicidin; Ebihara et al., 1995, Kyrozis and Reichling, 1995), thus making electrical contact with the cell interior, avoids these problems to a large extent. Nevertheless, cytoplasmic isolation is not complete, and problems such as an imperfect space-clamp (Müller and Lux, 1993) persist. In contrast, V_m measurements based on cell-attached K^+ current reversal concerns the local potential at the site of the patch, whereas V_m of the attached cell is not clamped and able to show unrestrained physiological fluctuations. The point nature of this type of measurement may eventually prove useful to study possible regional variations in V_m over the neuronal membrane.

Measurements of GABA actions on hippocampal interneurons

Actions of the neurotransmitter GABA depend crucially on the intracellular activities of Cl^-, HCO_3^-, and K^+ ions. For example, concentration shifts of these ions are thought to occur during prolonged GABAergic stimulation (see below). Because it does not perturb the cytoplasm, a cell-attached approach to determine V_m is particularly well suited to explore GABA actions. Although the time resolution of this technique (limited to ~1 Hz) did not permit individual synaptic events to be resolved, the effects on V_m of exogenous applied GABA or selective agonists for $GABA_A$ and $GABA_B$ receptors are easily detected.

We found that bath-applied GABA stabilized the V_m of interneurons at a level similar to its control value in slices from animals aged 1–3 weeks. Dissection of this response using selective agonists suggested that the membrane stabilization represented a balance between a hyperpolarizing action via $GABA_B$ receptors and a depolarization mediated by $GABA_A$ receptor activation. In contrast, in animals aged 1–4 d, the $GABA_B$ receptor agonist baclofen had no effect, as observed also in CA3 pyramidal cells at a similar developmental stage (Strata and Cherubini, 1994; Gaiarsa et al., 1995), and the depolarizing $GABA_A$-mediated response predominated. Even in P1–P4 animals the $GABA_A$-dependent depolarization rarely induced cell firing, as judged by

an absence of action currents from cell-attached records. The stabilization of V_m induced by GABA in neurons from older animals, and to a lesser extent also young animals, presumably reflects the shunting of the cell membrane by the GABA-activated conductances (Staley and Mody, 1992; Zhang and Jackson, 1993).

The origin of depolarizing responses to $GABA_A$ receptor activation remains to be completely understood. In this study, muscimol depolarized CA1 interneurons to similar membrane potentials, close to −55 mV, in animals from all ages that we examined (Fig. 5). There are numerous reports of biphasic $GABA_A$ responses generated in pyramidal cells, either by repetitive synaptic stimulation or by applying exogenous GABA. These responses consist of a short initial hyperpolarization, followed by a prolonged depolarization (Alger and Nicoll, 1979; Staley et al., 1995; Kaila et al., 1997). It seems probable that the time resolution of our method was not sufficient to capture the initial hyperpolarization and that we largely recorded the depolarizing component of the response. This component may result from an activity-dependent collapse of the Cl^- gradient after which the HCO_3^- current through the $GABA_A$ channel becomes dominant (Staley et al., 1995) analogous to the mechanism in crayfish muscle (Kaila et al., 1989). An additional depolarization may result from an increase in extracellular $[K^+]$ (Barolet and Morris, 1991) because of the activity in other interneurons (Kaila et al., 1997), although our results showing that GABA did not enhance cell firing might argue against this.

The observation that muscimol depolarizes V_m of CA1 interneurons in young and old animals to exactly the same level could suggest that the Cl^- reversal potential is the same for both age groups, in contrast to what has been suggested for hippocampal pyramidal cells (Mueller et al., 1984; Ben-Ari et al., 1989), and that in interneurons age-related changes in GABAergic action arise primarily from a change in functional receptor repertoire. However, the possible ionic shifts associated with the prolonged GABAergic stimulation in the present experiments precludes a reliable estimation of resting levels of intracellular ions, and other experiments in which ion shifts are somehow controlled are needed to specifically address the question of developmental changes in Cl^- homeostasis.

In this study we assessed the effects of GABA receptor activation on V_m from the reversal of somatic K^+ fluxes. This approach yields a point potential at the somatic patch, which may differ from that at other membrane surface sites (Spruston and Johnston, 1992). It might be especially interesting to use this technique to look for differences between somatic and dendritic responses to GABA receptor activation (Misgeld et al., 1986; Staley et al., 1995; Kaila et al., 1997).

REFERENCES

Alger BE, Nicoll RA (1979) GABA-mediated biphasic inhibitory responses in hippocampus. Nature 281:315–317.

Barolet AW, Morris ME (1991) Changes in extracellular K^+ evoked by GABA, THIP, and baclofen in the guinea-pig hippocampal slice. Exp Brain Res 84:591–598.

Barry PH, Lynch JW (1991) Liquid junction potentials and small cell effects in patch-clamp analysis. J Membr Biol 121:101–117.

Ben-Ari Y, Cherubini E, Corradetti R, Gaiarsa J-L (1989) Giant synaptic potentials in immature rat CA3 hippocampal neurones. J Physiol (Lond) 416:303–325.

Bormann J, Hamill OP, Sakmann B (1987) Mechanism of anion permeation through channels gated by glycine and γ-aminobutyric acid in mouse cultured spinal neurones. J Physiol (Lond) 385:243–286.

Chen G, Trombley PQ, van den Pol AN (1996) Excitatory actions of GABA in developing rat hypothalamic neurones. J Physiol (Lond) 494:451–464.

Ebihara S, Shirato K, Harata N, Akaike N (1995) Gramicidin-perforated patch recording: GABA response in mammalian neurones with intact intracellular chloride. J Physiol (Lond) 484:77–86.

Gaiarsa J-L, Tseeb V, Ben-Ari Y (1995) Postnatal development of pre- and postsynaptic $GABA_B$-mediated inhibitions in the CA3 hippocampal region of the rat. J Neurophysiol 73:246–255.

Gray R, Johnston D (1985) Rectification of single GABA-gated chloride channels in adult hippocampal neurons. J Neurophysiol 54:134–142.

Hille B (1992) Ionic channels of excitable membranes, Ed 2. Sunderland, MA: Sinauer.

Horn R, Marty A (1988) Muscarinic activation of ionic currents measured with a new whole-cell recording method. J Gen Physiol 92:145–159.

Kaila K, Pasternack M, Saarikoski J, Voipio J (1989) Influence of GABA-gated bicarbonate conductance on membrane potential, current, and intracellular chloride in crayfish muscle fibers. J Physiol (Lond) 416:161–181.

Kaila K (1994) Ionic basis of $GABA_A$ receptor channel function in the nervous system. Prog Neurobiol 42:489–537.

Kaila K, Lamsa K, Smirnov S, Taira T, Voipio J (1997) Long-lasting GABA-mediated depolarization evoked by high-frequency stimulation in pyramidal neurons of rat hippocampal slice is attributable to a network-driven, bicarbonate-dependent K^+ transient. J Neurosci 17:7662–7672.

Kyrozis A, Reichling DB (1995) Perforated-patch recording with gramicidin avoids artifactual changes in intracellular chloride concentration. J Neurosci Methods 57:27–35.

Lynch JW, Barry PH (1989) Action potentials initiated by single channels opening in a small neuron (rat olfactory receptor). Biophys J 55:755–768.

Marty A, Neher E (1995) Tight-seal whole-cell recording. In: Single channel recording (Sakmann B, Neher E, eds), pp 31–52. New York: Plenum.

Michelson HB, Wong RKS (1991) Excitatory synaptic responses mediated by $GABA_A$ receptors in the hippocampus. Science 253:1420–1423.

Misgeld U, Deisz RA, Dodt HU, Lux HD (1986) The role of chloride transport in postsynaptic inhibition of hippocampal neurons. Science 232:1413–1415.

Mueller AL, Taube JS, Schwartzkroin PA (1984) Development of hyperpolarizing inhibitory postsynaptic potentials and hyperpolarizing response to γ-aminobutyric acid in rabbit hippocampus studied *in vitro*. J Neurosci 4:860–867.

Müller W, Lux HD (1993) Analysis of voltage-dependent membrane currents in spatially extended neurons from point-clamp data. J Neurophysiol 69:241–247.

Neher E (1992) Correction for liquid junction potentials in patch-clamp experiments. In: Ion channels; Methods in enzymology, Vol 207, pp 123–131. New York: Academic.

Ohno-Shosaku T, Yamamoto C (1992) Identification of an ATP-sensitive K^+ channel in rat cultured cortical neurons. Pflügers Arch 422:260–266.

Otis TS, De Koninck Y, Mody I (1993) Characterization of synaptically elicited $GABA_B$ responses using patch-clamp recordings in rat hippocampal slices. J Physiol (Lond) 463:391–407.

Owens DF, Boyce LH, Davis MB, Kriegstein AR (1996) Excitatory GABA responses in embryonic and neonatal cortical slices demonstrated by gramicidin perforated-patch recordings and calcium imaging. J Neurosci 16:6414–6423.

Ozawa S, Yuzaki M (1984) Patch-clamp studies of chloride channels activated by gamma-aminobutyric acid in cultured hippocampal neurones of the rat. Neurosci Res 1:275–293.

Parra P, Gulyas AI, Miles R (1998) How many subsets of inhibitory cells in the hippocampus? Neuron 20:983–993.

Sakura H, Ammala C, Smith PA, Gribble FM, Ashcroft FM (1995) Cloning and functional expression of the cDNA encoding a novel ATP-sensitive potassium channel subunit expressed in pancreatic beta-cells, brain, heart and skeletal muscle. FEBS lett 377:338–344.

Soltesz I, Mody I (1994) Patch-clamp recordings reveal powerful GABAergic inhibition in dentate hilar neurons. J Neurosci 14:2365–2376.

Spruston N, Johnston D (1992) Perforated patch-clamp analysis of the passive membrane properties of three classes of hippocampal neurons. J Neurophysiol 67:508–529.

Staley KJ, Mody I (1992) Shunting of excitatory input to dentate gyrus granule cells by a depolarizing $GABA_A$ receptor-mediated postsynaptic conductance. J Neurophysiol 68:197–212.

Staley KJ, Soldo BL, Proctor WR (1995) Ionic mechanisms of neuronal excitation by inhibitory $GABA_A$ receptors. Science 269:977–981.

Strata F, Cherubini E (1994) Transient expression of a novel type of GABA response in rat CA3 hippocampal neurones during development. J Physiol (Lond) 480:493–503.

Strata F, Atzori M, Molnar M, Ugolini G, Tempia F, Cherubini E (1997) A pacemaker current in dye-coupled hilar interneurons contributes to the generation of giant GABAergic potentials in developing hippocampus. J Neurosci 17:1435–1446.

Thompson SM, Gähwiler BH (1989) Activity-dependent disinhibition, I: repetitive stimulation reduces IPSP driving force and conductance in the hippocampus *in vitro*. J Neurophysiol 61:501–511.

Verheugen JAH, Vijverberg HPM (1995) Intracellular Ca^{2+} oscillations and membrane potential fluctuations in intact human T lymphocytes: role of K^+ channels in Ca^{2+} signaling. Cell Calcium 17:287–300.

Verheugen JAH, Vijverberg HPM, Oortgiesen M, Cahalan MD (1995) Voltage-gated and Ca^{2+}-activated K^+ channels in intact human T lymphocytes: non-invasive measurements of membrane currents, membrane potential, and intracellular calcium. J Gen Physiol 105:765–794.

Verheugen JAH, Korn H (1997) A charybdotoxin-insensitive potassium conductance in human T lymphocytes: T cell membrane potential is set by distinct K^+ channels. J Physiol (Lond) 503:317–331.

Whittington MA, Traub RD, Jefferys JGR (1995) Synchronized oscillations in interneuron networks driven by metabotropic glutamate receptor activation. Nature 373:612–615.

Zhang L, McBain CJ (1995) Voltage-gated potassium currents in stratum oriens-alveus inhibitory neurones of the rat CA1 hippocampus. J Physiol (Lond) 488:647–660.

Zhang L, Spigelman I, Carlen PL (1991) Development of GABA-mediated, chloride-dependent inhibition in CA1 pyramidal neurones of immature rat hippocampal slices. J Physiol (Lond) 444:25–49.

Zhang SJ, Jackson MB (1993) GABA-activated chloride channels in secretory nerve endings. Science 259:531–534.